ISSN 1063-7834, Physics of the Solid State, 2016, Vol. 58, No. 5, pp. 908–914. © Pleiades Publishing, Ltd., 2016.
Original Russian Text © A.S. Parshin, A.Yu. Igumenov, Yu.L. Mikhlin, O.P. Pchelyakov, V.S. Zhigalov, 2016, published in Fizika Tverdogo Tela, 2016, Vol. 58, No. 5, pp. 881–887.

METALS

Comparative Analysis of Characteristic Electron Energy Loss Spectra and Inelastic Scattering Cross-Section Spectra of Fe

A. S. Parshin[a, *], A. Yu. Igumenov[a], Yu. L. Mikhlin[b], O. P. Pchelyakov[c], and V. S. Zhigalov[d]

[a] *Siberian State Aerospace University, ul. Gazety Krasnoyarskii Rabochii 31, Krasnoyarsk, 660014 Russia*
[b] *Institute of Chemistry and Chemical Technology, Siberian Branch, Russian Academy of Sciences, Akademgorodok 50/24, Krasnoyarsk, 660036 Russia*
[c] *Rzhanov Institute of Semiconductor Physics, Siberian Branch, Russian Academy of Sciences, pr. Akademika Lavrent'eva 13, Novosibirsk, 630090 Russia*
[d] *Kirensky Institute of Physics, Siberian Branch, Russian Academy of Sciences, Akademgorodok 50/38, Krasnoyarsk, 660036 Russia*
**e-mail: aparshin2010@mail.ru*

Received July 15, 2015; in final form, October 28, 2015

Abstract—The inelastic electron scattering cross section spectra of Fe have been calculated based on experimental spectra of characteristic reflection electron energy loss as dependences of the product of the inelastic mean free path by the differential inelastic electron scattering cross section on the electron energy loss. It has been shown that the inelastic electron scattering cross-section spectra have certain advantages over the electron energy loss spectra in the analysis of the interaction of electrons with substance. The peaks of energy loss in the spectra of characteristic electron energy loss and inelastic electron scattering cross sections have been determined from the integral and differential spectra. It has been shown that the energy of the bulk plasmon is practically independent of the energy of primary electrons in the characteristic electron energy loss spectra and monotonically increases with increasing energy of primary electrons in the inelastic electron scattering cross-section spectra. The variation in the maximum energy of the inelastic electron scattering cross-section spectra is caused by the redistribution of intensities over the peaks of losses due to various excitations. The inelastic electron scattering cross-section spectra have been analyzed using the decomposition of the spectra into peaks of the energy loss. This method has been used for the quantitative estimation of the contributions from different energy loss processes to the inelastic electron scattering cross-section spectra of Fe and for the determination of the nature of the energy loss peaks.

DOI: 10.1134/S106378341605019X

1. INTRODUCTION

Iron is one of the most promising materials for nanoelectronics, spintronics, and photonics [1–3]. Multilayered Fe/Si structures are interesting for theoretical and practical applications [1–3], and are being intensively studied by various methods. One of the most popular methods for the analysis of nanomaterials is electron spectroscopy. In this work, we have performed a detailed analysis of the characteristic electron energy loss spectra (EELS) and inelastic electron scattering cross-section spectra ($K\lambda$-spectra) of Fe.

The interest in inelastic electron scattering cross-section spectroscopy is caused by the fact that, in contrast to the initial spectra of the characteristic reflection electron energy loss, the $K\lambda$-spectra are free from the loss due to multiple excitations and the intensity is expressed in absolute units. These spectra are also more sensitive to variations in the energy of primary electrons and the emission angle [4–6]. The inelastic electron scattering cross-section spectroscopy makes it possible to determine the elemental composition with a significantly higher accuracy than the traditional reflection electron energy loss spectroscopy [7].

The inelastic electron scattering cross-section spectra are calculated on the basis of experimental reflection electron energy loss spectra and make possible the quantitative analysis of the elemental composition of two-component composite structures. Earlier, the possibility of quantitative determination of atomic concentration of elements from the maximum in the $K\lambda$-spectra in Fe_xSi_{1-x} [8, 9], Mn_xSi_{1-x} [7], and Ge_xSi_{1-x} systems was studied [10].

Computer simulation of the inelastic electron scattering cross-section spectra in the framework of the dielectric theory was applied for the analysis of distribution of elements through depth, the formation of different phases of silicides in the Fe/Si system [9], and for determining the thickness of the silicon dioxide on the surface of a silicon substrate [11].

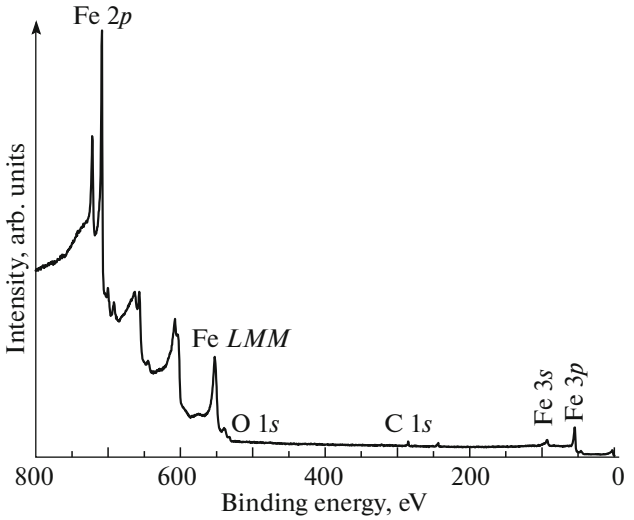

Fig. 1. Panoramic XPS of the Fe film on the Si substrate.

In this work, we have performed a comparative analysis of the characteristic reflection electron energy loss and inelastic electron scattering cross-section spectra of Fe. The maximum energy in the inelastic electron scattering cross-section spectra depends on the intensities of its peaks, which manifests itself in experimental $K\lambda$-spectra and is confirmed by the simulation of spectra by the superposition of two peaks with close energies.

For the analysis of the inelastic electron scattering cross-section spectra of Fe, we applied for the first time our method [12, 13] making possible a quantitative estimation of contributions from different energy loss processes to the inelastic electron scattering cross-section spectra.

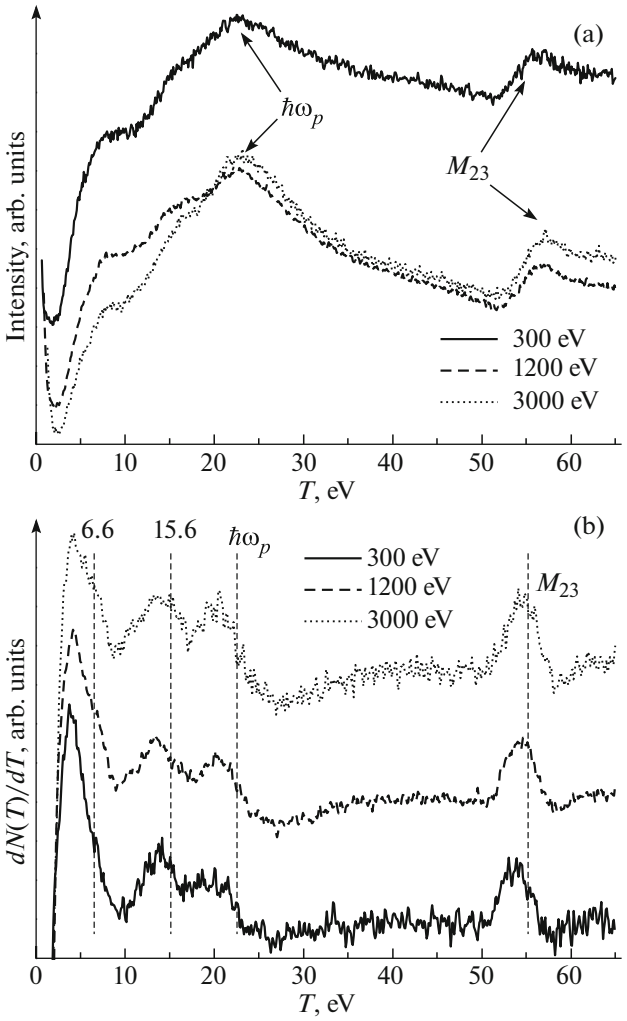

Fig. 2. Fe EELS normalized to the elastic peak in the (a) integral and (b) differential forms.

2. SAMPLE PREPARATION AND EXPERIMENTAL TECHNIQUE

The Fe samples were fabricated by high-vacuum thermal evaporation. Three samples were studied: a bulk Fe sample, a 50 nm-thick Fe film on a Si substrate, and a 50 nm-thick Fe film on a glass substrate.

Measurements of the photoelectron spectra and integral reflection electron energy loss spectra were performed on a SPECS (Germany) ultra-high-vacuum photoelectron spectrometer at the incidence and detection angles with the normal to the sample surface of $\alpha_i = 59°$ and $\alpha_d = 0°$, respectively. The spectrometer was supplied with a PHOIBOS MCD9 spherical energy analyzer, an X-ray tube with a double anode as the X-ray source, and a Microfocus EK-12-M (STAIB Instruments) electron-beam projector for excitation of electron energy loss spectra. Surface impurities and protective and oxide layers were removed by Ar^+-ion etching (an accelerating voltage of 2.5 kV and an ion current of 15 μA) with a PU-IQE-12/38 (SPECS) scanning ion gun in the spectrometer chamber before recording the electron spectra. The completeness of the removal of oxygen and impurities was controlled from X-ray photoelectron spectra (XPS): the degree of oxygen and carbon contamination after the Ar^+-ion etching was on the order of 5%. Figure 1 shows the panoramic XPS of Fe on a Si substrate, in which photoelectron peaks and Auger peaks are marked.

3. EXPERIMENTAL RESULTS AND DISCUSSION

3.1. Characteristic Electron Energy Loss Spectroscopy

Experimental spectra of characteristic reflection electron energy losses were obtained in the interval of 0–150 eV with a step of 0.1 eV. The energy loss T was calculated as the difference between the energy of primary electrons, E_0, (zero loss) and the energy of reflected electrons, E: $T = E_0 - E$. The energies of primary electrons were 300, 600, 1200, 1900, and 3000 eV.

Table 1. Energies of peaks (in eV) in EELS

E_0, eV	Integral EELS		Differential EELS			
	$\hbar\omega_p$	M_{23}	peak 1	peak 2	$\hbar\omega_p$	M_{23}
300	22.75	56.11	5.93	15.36	22.81	55.46
600	22.46	56.78	6.47	15.44	22.77	55.98
1200	22.74	56.52	7.01	15.42	22.79	55.87
1900	22.93	56.91	6.80	15.70	22.90	55.74
3000	22.93	57.05	6.88	16.24	22.89	56.03
Mean value	22.76	56.68	6.62	15.63	22.83	56.21
Deviation	0.19	0.37	0.43	0.36	0.38	0.23

The EELS of three Fe samples differed insignificantly. Figure 2 shows the spectra averaged over three samples in the integral (a) and differential (b) forms. In the integral spectra, we observe well-resolved peaks at the loss energies about 22.8 and 56.7 eV and small peaks in the low-loss region, the energy of which is difficult to determine. The peak at 22.8 eV, apparently, is connected with the excitation of the bulk plasmon in Fe (in the generally accepted notation, $\hbar\omega_p$) and is close to data published in [14–18], and the peak at 56.7 eV corresponds to the M_{23} interband transition [14, 15, 17–20]. The energies of the loss peaks were determined from the integral and differential EELS and are presented in Table 1. The differentiation of EELS makes it possible to subtract the structureless background and determine the energies of small peaks (Fig. 2b). The peak at 15.6 eV (peak *2* in Table 1), apparently, corresponds to the excitation of the surface plasmon in Fe, and its energy is close to publishes values [17, 18]; the peak at 6.6 eV (peak *1* in Table 1) corresponds to an interband transition [16]. As is evident from Table 1, the energy of the bulk plasmon in the integral and differential EELS is practically independent of the energy of primary electrons. With an increase in the energy of primary electrons, the contribution of the bulk plasmon relative to the poorly resolved peaks in the low-energy region containing the surface plasmon increases (Fig. 2).

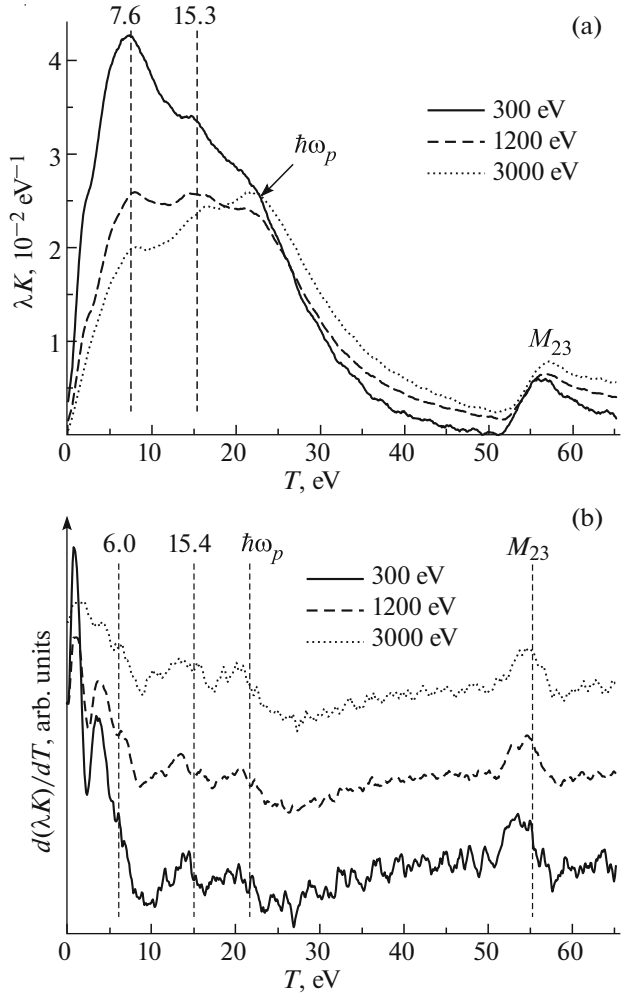

Fig. 3. Inelastic electron scattering cross-section spectra of Fe in the (a) integral and (b) differential forms.

3.2. Inelastic Electron Scattering Cross-Section Spectroscopy

From experimental reflection electron energy loss spectra, with the help of the QUASES™ XS REELS (quantitative analysis of surfaces by electron spectroscopy cross sections determined by REELS) software package [21], by the algorithm suggested in [22], the inelastic electron scattering cross section was obtained as the product of the electron inelastic mean free path λ by the differential inelastic electron scattering cross section $K(E_0, E_0 - E)$ (Fig. 3a). The inelastic electron scattering cross-section spectra reflect the probability of the energy loss T by an electron in a single scattering in the inelastic mean free path per unit energy. The maxima of these spectra determine the probability of a single energy loss due to surface and bulk excitations. The absolute values of the energy loss in inelastic electron scattering cross-section spectra make possible the comparison and analysis of spectra of different materials (including those obtained by different authors) without preprocessing and normalization.

The inelastic electron scattering cross-section spectra of Fe are close to those presented in [23, 24]. In the $K\lambda$-spectra of Fe (Fig. 3a) as compared to the EELS, the peak at the energy of 15.3 eV (peak *3* in Table 2), which corresponds to the excitation of a surface plasmon in Fe [17, 18], is resolved better and is more intense. Peak *2* in the $K\lambda$-spectra (Table 2) is close in the energy to peak *1* in the differential EELS (Table 1) and corresponds to an interband transition [16]. In the $K\lambda$-spectra, this peak is resolved better and

Table 2. Energies of peaks (in eV) in $K\lambda$-spectra

E_0, eV	Integral $K\lambda$-spectra				Differential $K\lambda$-spectra				
	peak 2	peak 3	$\hbar\omega_p$	M_{23}	peak 1	peak 2	peak 3	$\hbar\omega_p$	M_{23}
300	7.06	14.68		55.73	1.67	5.92	14.90	21.89	55.03
600	7.47	14.49		56.15	1.85	5.82	15.21	22.19	55.55
1200	7.78	15.18	21.21	56.08	1.79	6.12	15.22	22.58	55.52
1900	7.71	15.93	21.67	56.30	2.11	6.29	15.71	22.74	55.84
3000	8.08	16.23	21.67	56.68	2.68	6.08	15.80	22.75	55.74
Mean value	7.62	15.30	21.51	56.19	2.02	6.05	15.37	22.43	55.54
Deviation	0.38	0.76	0.27	0.35	0.40	0.18	0.38	0.38	0.31

is more intense than that in the EELS. The intensity of the loss due to surface excitations in the $K\lambda$-spectra is higher than in the EELS, because the Tougaard–Chorkendorff algorithm [22] presumes the subtraction of the background and removal of multiple plasma losses. In addition, the $K\lambda$-spectra of Fe exhibit peaks at the energies close to those in the EELS (21.5 and 56.2 eV), which correspond to the losses due to the excitation of the bulk plasmon $\hbar\omega_p$ and the M_{23} interband transition.

The variation in the shape of the inelastic electron scattering cross-section spectra with an increase in the energy of primary electrons is caused by the increase in the escape depth of reflected electrons, which results in an increase in the intensity of bulk excitations and a reduction in the intensity of surface excitations. From the comparison of the EELS and inelastic electron scattering cross-section spectra, it follows that the shape of the $K\lambda$-spectra is more subjected to changes due to variations in the intensity of primary electrons.

For a more accurate determination of the energy loss peaks, numerical differentiation of the $K\lambda$-spectra was performed (Fig. 3b). The energies of peaks in the inelastic electron scattering cross-section spectra of Fe were determined from the integral and differential spectra and are presented in Table 2. The differentiation of the inelastic electron scattering cross-section spectra, as well as EELS, made it possible to determine the energies of small peaks. The energy loss of the peaks $\hbar\omega_p$, M_{23}, and peak *3* are close to those determined from EELS and from published data on EELS [14–20] and $K\lambda$-spectra [25]. Peak *1* at 2.02 eV (Table 2) corresponds to a one-electron transition from the top of the Fe 3*d* band to unoccupied states 1.5 eV above E_F [17, 18], and peak *2* at 6.05 eV, to the interband transition [16], which is also observed in the differential EELS.

The energy of the bulk plasmon is practically independent of the energy of primary electrons in the EELS and monotonically increases with increasing energy of primary electrons in the inelastic electron scattering cross-section spectra (Fig. 4). The mean energy of the bulk plasmon determined from the differential EELS, is 22.8 ± 0.1 eV; it is practically independent of the energy of primary electrons. The energy of the bulk plasmon determined from the differential inelastic electron scattering cross-section spectra as a function of the energy of primary electrons is approximated well by the exponential function and asymptotically tends to 22.8 eV, which equals the mean value determined from the EELS.

This result demonstrates a high sensitivity of the inelastic electron scattering cross-section spectra to variations in the energy of primary electrons. Since the $K\lambda$-spectrum is a superposition of different processes of inelastic electron scattering, the variation in the energy of the bulk plasmon in the $K\lambda$-spectra may be connected with the redistribution of intensity over peaks of energy losses due to surface and bulk excitations.

In order to confirm the influence of the relationship between the intensities of peaks in the spectrum,

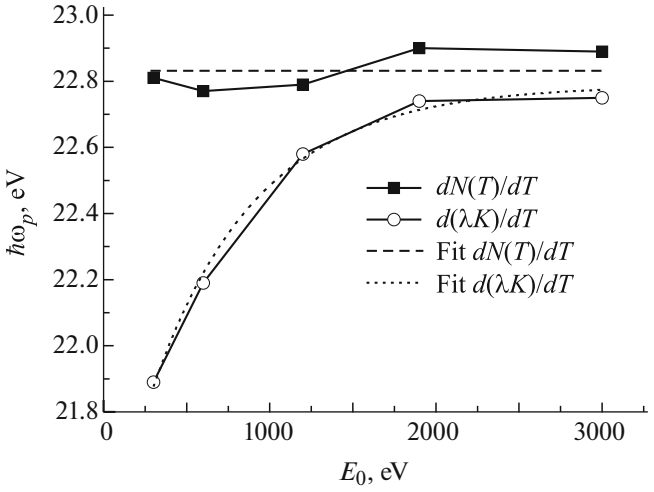

Fig. 4. Energy of the bulk plasmon determined from EELS and inelastic electron scattering cross-section spectra vs. the energy of primary electrons.

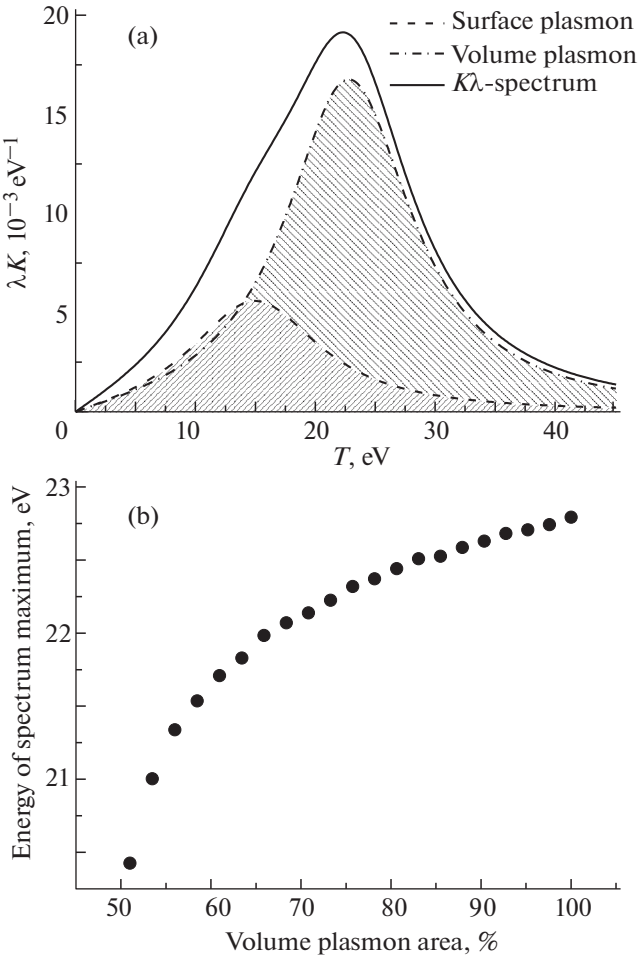

Fig. 5. (a) Model $K\lambda$-spectrum consisting of two peaks with the relative fraction of the area of the high-energy peak of 76% and (b) the energy of the maximum of the model spectrum vs. the relative fraction of the area of the high-energy peak.

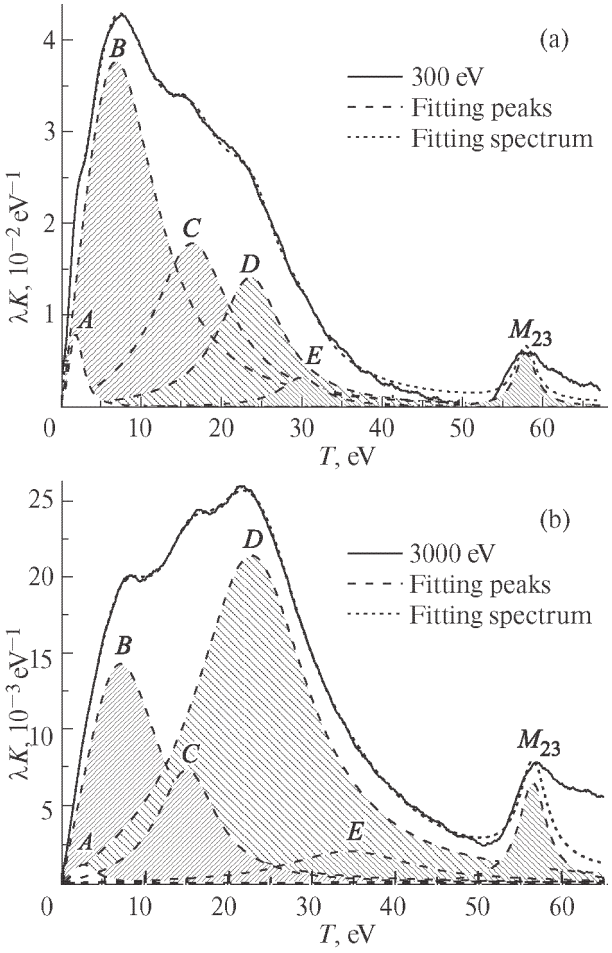

Fig. 6. Inelastic electron scattering cross-section spectra of Fe for primary electron energies of (a) 300 and (b) 3000 eV, approximated by Lorentz-like Tougaard functions.

the $K\lambda$-spectrum was simulated by a sum of two unresolved peaks. The shape of the peaks was described by Lorentz-like Tougaard functions [23]

$$\lambda K = \frac{\mathcal{B}T}{(\mathcal{C} - T^2)^2 + \mathcal{D}T^2}.$$

Here, $\mathcal{B}$, $\mathcal{C}$, and $\mathcal{D}$ are fitting parameters, which have definite values for each element [23]. Parameter $\mathcal{B}$ determines the intensity of the peak, parameter $\mathcal{C}$ determines its position, and parameter $\mathcal{D}$ determines its width and indirectly influences the position and intensity of the peak. The description of inelastic electron scattering cross-section spectra by Lorentz-like function (universal classes of the inelastic electron scattering cross sections) was proposed by Tougaard [23].

We chose peaks of the same width and the energy losses close to the energies of the surface and bulk plasmons in Fe: 14.9 and 22.8 eV.

Figure 5a shows the resulting spectrum with the areas of the peaks in its composition relating as 24 and 76%. The peaks are practically unresolved in the energy, and the position of the maximum differs from the position of the dominant peak. With an increase in the intensity of the high-energy peak, the maximum of the resulting spectrum shifts toward the dominant peak (Fig. 5b). This dependence tends to the energy of the high-energy peak.

Thus, the loss energy of the peak corresponding to the excitation of the bulk plasmon can be determined with a higher confidence than the energy of other peaks, because in this case we may eliminate the influence of the intensities of different contributions on the resulting position of the maximum in the spectrum.

3.3. Approximation of the Inelastic Electron Scattering Cross-Section Spectra by the Tougaard Universal Functions

For the quantitative estimation of the variation in the contributions of different nature to the inelastic

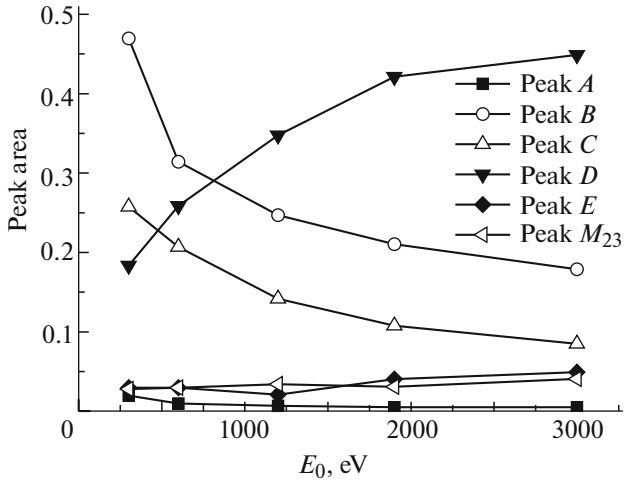

Fig. 7. Areas of the fitting peaks vs. the energy of primary electrons.

electron scattering cross-section spectra, it was proposed in [13, 14] to approximate the spectrum by the three-parameter Tougaard functions [23]. The study of the processes of electron energy loss by separating contributions of different nature from inelastic electron scattering cross-section spectra is an urgent problem of electron spectroscopy, which can be used for estimating the influence of surface excitations on EELS, XPS, and Auger-electron spectra [4–6, 25–28].

Figure 6 shows the result of approximation of the inelastic electron scattering cross-section spectra of Fe at the energy of primary electrons of 300 (Fig. 6a) and 3000 eV (Fig. 6b). The number of fitting peaks was chosen from the condition of the minimum root-mean-square deviation of the fitting spectrum from the experimental one. For a good approximation, it suffices six peaks, including M_{23}.

The inelastic electron scattering cross-section spectra of Fe were approximated by six Tougaard peaks: peaks A, B, C, D, E, and M_{23}. Parameters $\mathcal{B}$, $\mathcal{C}$, and $\mathcal{D}$ of the Tougaard function were varied until reaching the best agreement between the fitting and experimental spectra. In the approximation, the energy of peak D (bulk plasmon) was set as equal to the mean energy determined from the EELS for the bulk plasmon (22.8 eV).

It is evident from Fig. 6 that, with an increase in the energy of primary electrons, the intensity of peak D increases and the intensities of peaks A, B, and C decrease. The variation in the intensities of separate peaks causes variation in the shape of the whole spectrum. The decomposition of the inelastic electron scattering cross-section spectra into loss peaks makes it possible to estimate the contributions of separate processes to the resulting $K\lambda$-spectrum.

Figure 7 shows the dependence of the area of fitting peaks, which determines the intensities of excitations, on the energy of primary electrons. The monotonically decreasing dependences of peaks B and C evidence their surface nature, and the opposite tendency in the dependence of the area of peak D evidences its bulk nature. The nature of the other peaks is hard to determine uniquely because of their low intensity. The mean energies of the fitting peaks and the root-mean-square deviations are presented in Table 3.

The energies of peak C in the approximation was freely varied and, as a result, took a value close to the published data for the surface plasmon in Fe [17, 18] and the ratio of the energy loss of the bulk plasmon to the energy loss of peak C is close to $\sqrt{2}$, which is well-known from the classical plasmon theory for free electron gas [29].

The energy of peak B, obtained as a result of the approximation, is close to the energy of experimental peaks in the EELS and $K\lambda$-spectra.

The energy of peak A varies from 1.6 to 2.6 eV as the energy of primary electrons varies from 300 to 3000 eV, as well as the energy of this peak determined from differential $K\lambda$-spectra (Table 2). Thus, peak A can comprise two unresolved peaks: surface-like and bulk-like ones. In this case, the energy loss of the surface-like peak is lower than that of the bulk-like one. The mean energy of peak A is close to the energy of peak *1* in the differential inelastic electron scattering cross-section spectra of Fe (Table 2). With an increase in the energy of free electrons, the intensity of the bulk-like peak increases and the position of the resulting peak A shifts to the high-energy region.

Table 3. Energies of fitting peaks (in eV)

E_0, eV	A	B	C	D	E	M_{23}
300	1.60	6.55	15.73	22.80	28.98	56.07
600	1.75	6.70	15.15	22.80	31.17	56.36
1200	1.75	6.99	15.00	22.80	34.52	56.51
1900	1.89	6.99	15.00	22.80	35.25	56.51
3000	2.62	7.14	15.00	22.80	34.66	56.66
Mean value	1.92	6.87	15.18	22.80	32.92	56.42
Deviation	0.40	0.24	0.32	0.00	2.72	0.22

4. CONCLUSIONS

The characteristic electron energy loss spectra and inelastic electron scattering cross-section spectra of Fe were studied. The comparative analysis demonstrated the advantages of inelastic electron scattering cross-section spectra for the quantitative analysis of the interaction of electrons with matter over the EELS. The fine structure of the inelastic electron scattering cross-section spectra was studied by the approximation of the experimental spectra by three-parameter Tougaard functions. A quantitative estimation of the

contributions of different inelastic electron scattering processes to the $K\lambda$-spectra of Fe obtained at different energies of primary electrons was performed. The nature of the loss peaks was determined from the dependence of their intensity on the energy of primary electrons.

This method can be used for the analysis of mechanisms of electron scattering and quantitative estimation of the contributions of separate scattering processes to the inelastic electron scattering cross-section spectra of various materials.

REFERENCES

1. N.G. Galkin, D.L. Goroshko, E. A. Chusovitin, K. N. Galkin, and S. A. Dotsenko, Phys. Status Solidi C **10** (12), 1670 (2013).
2. Y. Maeda and Y. Terai, in *Proceedings of the International Meeting for Future of Electron Devices (IMFEDK-2004), Kyoto University, Kyoto, Japan, July 26–28, 2004* (Institute of Electrical and Electronics Engineers (IEEE), Piscataway, New Jersey, 2004), p. 67.
3. H. Tokushige, T. Endo, K. Hiidome, K. Saiki, S. Kitamura, T. Katsuyama, N. Ikeda, Y. Sugimoto, and Y. Maeda, Jpn. J. Appl. Phys. **54**, 07JB03 (2015).
4. H. Jin, H. Yoshikawa, H. Iwai, S. Tanuma, and S. Tougaard, J. Surf. Anal. **15** (3), 321 (2009).
5. H. Jin, H. Shinotsuka, H. Yoshikawa, H. Iwai, S. Tanuma, and S. Tougaard, J. Appl. Phys. **107**, 083709 (2010).
6. H. Jin, H. Shinotsuka, H. Yoshikawa, H. Iwai, M. Arai, S. Tanuma, and S. Tougaard, Surf. Interface Anal. **45** (6), 985 (2013).
7. A. S. Parshin, O. P. Pchelyakov, A. E. Dolbak, and B. Z. Ol'shanetskii, J. Surf. Invest. **7** (3), 505 (2013).
8. A. S. Parshin, G. A. Alexandrova, A. E. Dolbak, O. P. Pchelyakov, B. Z. Ol'shanetskii, S. G. Ovchinnikov, and S. A. Kushchenkov, Tech. Phys. Lett. **34** (5), 381 (2008).
9. A. S. Parshin, S. A. Kushchenkov, G. A. Aleksandrova, and S. G. Ovchinnikov, Tech. Phys. **56** (5), 656 (2011).
10. A. C. Parshin, E. P. P'yanovskaya, O. P. Pchelyakov, Yu. L. Mikhlin, A. I. Nikiforov, B. A. Timofeev, and M. Yu. Esin, Semiconductors **48** (2), 224 (2014).
11. A. S. Parshin, S. A. Kushchenkov, O. P. Pchelyakov, Yu. L. Mikhlin, and T. Khasanov, Avtometriya **48** (4), 88 (2012).
12. A. S. Parshin, A. Yu. Igumenov, Yu. L. Mikhlin, O. P. Pchelyakov, A. I. Nikiforov, and V. A. Timofeev, Semiconductors **49** (4), 423 (2015).
13. A. Yu. Igumenov, A. S. Parshin, Yu. L. Mikhlin, O. P. Pchelyakov, A. I. Nikiforov, and V. A. Timofeev, Vestn. Sib. Gos. Aerokosm. Univ. **56** (4), 230 (2014).
14. B. Egert and G. Panzner, Phys. Rev. B: Condens. Matter **29** (4), 2091 (1984).
15. Y. Sakisaka, T. Myano, and M. Onchi, Phys. Rev. B: Condens. Matter **30** (12), 6849 (1984).
16. E. Colavita, M. de Crescenzi, L. Papagno, R. Scarmozzino, L. S. Caputi, R. Rosei, and E. Tosatti, Phys. Rev. B: Condens. Matter **25** (4), 2490 (1982).
17. B. Egert and G. Panzner, J. Phys. F: Met. Phys. **11**, L233 (1981).
18. V. G. Lifshits and Yu. V. Lunyakov, *EELS Spectra of Surface Phases on Silicon* (Dal'nauka, Vladivostok, 2004), p. 142 [in Russian].
19. C. Colliex, T. Manoubi, and C. Ortis, Phys. Rev. B: Condens. Matter **44** (20), 11402 (1991).
20. L. C. Feldman and J. W. Mayer, *Fundamentals of Surface and Thin Film Analysis* (Elsevier, New York, 1986).
21. S. Tougaard, http:// www.quases.com.
22. S. Tougaard and I. Chorkendorff, Phys. Rev. B: Condens. Matter **35** (13), 6570 (1987).
23. S. Tougaard, Surf. Interface Anal. **25** (3), 137 (1997).
24. S. Tougaard and J. Kraaer, Phys. Rev. B: Condens. Matter **43** (2), 1651 (1991).
25. G. Gergely, M. Menyhard, S. Gurban, A. Sulyok, J. Toth, D. Varga, and S. Tougaard, Solid State Ionics **141–142**, 47 (2001).
26. G. Gergely, Prog. Surf. Sci. **71** (31), 1 (2002).
27. G. T. Orosz, G. Gergely, S. Gurban, M. Menyhard, J. Toth, D. Varga, and S. Tougaard, Vacuum **71**, 147 (2003).
28. S. Tougaard, Surf. Interface Anal. **11** (9), 453 (1988).
29. H. Raether, *Surface Plasmons on Smooth and Rough Surfaces and on Gratings* (Springer-Verlag, Berlin, 1988).

Translated by E. Chernokozhin